Research Article Wiley Online Library ELECTROANALYSIS

doi.org/10.1002/elan.202200234

Determination of Mercury with a Miniature Sensor for Point-of-care Testing

Caterina Andreasi Bassi[+],[a] Zhizhen Wu[+],[a] Linda Forst,[b] and Ian Papautsky*[a]

Abstract: In developing countries, subsistence gold mining entails mixing metallic mercury with crushed sediments to extract gold. In this approach, the gold–mercury amalgam is heated to evaporate mercury and obtain gold. Thus, the highly volatile mercury can be absorbed through inhalation, resulting in adverse health effects. Urinalysis can be used to detect mercury, which is excreted in urine and feces, and correlate exposure with toxic effects. The current gold standard analytical methods are based on fluorescence or inductively coupled plasma mass spectrometry methods, but are expensive, time consuming, and are not easily accessible in countries where testing is needed. In this work, we report on a miniature electrochemical sensor that can rapidly detect mercury in urine at levels well below the US Biological Exposure Index (BEI) limit of 50 ppb (μg/L). The sensor is based on a thin-film gold electrode and anodic stripping voltammetry electroanalytical approach. The sensor successfully detected mercury at trace levels in urine, with a limit of detection of ~15 ppb Hg in the linear range of 20–80 ppb. With the low-cost disposable sensors and portable instrumentation, it is well suited for point-of-care applications.

Keywords: Electrochemical sensor · anodic stripping voltammetry · mercury determination · urine · point-of-care · thin film gold sensor

1 Introduction

One application of mercury (Hg) is in artisanal and small-scale gold mining (ASGM) [1] where elemental mercury and gold are mixed together to form an amalgam in order to extract gold from ore sediments [2]. The amalgam is heated to evaporate mercury and obtain gold, resulting in a mining method that is cheap, fast, and easy, but highly inefficient. The process also releases mercury fumes into the ambient environment and directly exposes workers to them. ASGM is a worldwide phenomenon that involves an estimated 15 million people, of which 3 million are women and children, across 70 countries primarily in Asia, Africa, South and Central America. In addition to exposing a large number of people to Hg fumes, ASGM contributes to over 37% of the total of global Hg emissions, making it the largest source of Hg pollution [2]. Exposure to Hg vapors often leads to mercury poisoning due to inhalation, which leads to Hg accumulating in the liver, brain, kidney and bone tissues [3], ultimately leading to impaired cognition, fine motor skills, speech, and language development in children. Thus, assessment of Hg exposure is urgently needed.

Assessment of Hg exposure can be done in both whole blood and urine since elemental mercury (Hg^0) oxidizes to mercuric mercury (Hg^{++}) once in the bloodstream after crossing the alveolar-capillary barrier in the lungs, and is then excreted in the urine and feces [4]. However, the half-life of elemental mercury in blood decreases rapidly in the days after exposure [5], making assessment of chronic exposure difficult. Further, blood sample collection maybe challenging due to the need for phlebotomy, and cold storage, and/or shipping requirements. Urine maybe more suitable for exposure assessment [6,7], with half-life of Hg in urine being 1–3 months [8], it may be suitable for assessment for both chronic and acute exposure. Further, urine is a non-invasive sample that is easy to collect, making it the ideal approach to assessing inorganic Hg intoxication.

Quantification of Hg is usually done by cold vapor atomic absorption spectroscopy (CVAAS) [9], cold vapor atomic fluorescence spectrometry (CVAFS) [10], or inductively coupled plasma mass spectrometry (ICP-MS) [11]. These techniques exhibit very low limits of detection, with studies reporting 10 ng/L for CVAFS [12], 100 ng/L [13] for CVAAS and 170 ng/L [14] for ICP-MS, and accurate quantitative assessment of Hg in a wide range of organic matrices. However, the high instrumentation costs and the need for trained personnel means that only centralized labs can perform such measurements. The need to ship the collected samples to these labs for analysis leads to time delays and increased costs. Thus,

[a] C. Andreasi Bassi,[+] Z. Wu,[+] I. Papautsky
Department of Biomedical Engineering, University of Illinois Chicago, IL
851 S. Morgan Street, 218 SEO
Chicago, IL 60607, USA
Tel: +1312.413.3800
E-mail: papauts@uic.edu
[b] L. Forst
Department of Public Health, University of Illinois Chicago, IL
Chicago, IL 60607, USA
[+] C.A.B. and Z.W. contributed equally to this work.

these conventional approaches are not optimal for rapid intervention on populations in low-income regions or developing countries [15].

Electrochemical analytical methods have emerged as viable alternatives to the classic spectroscopy and spectrometry approaches, offering more rapid analysis, simpler instrumentation, and lower cost, which is more suitable for point-of-care (POC) applications. Previous work on electrochemical detection of mercury relied on anodic stripping voltammetry (ASV), one of such techniques capable of limits of detection (LODs) in the sub-part-per-billion (μg/L) range [16,17]. The approach involves a pre-concentration step, during which the working electrode is biased at a potential to reduce target analyte until an adequate amount has been deposited, and a stripping step to oxidize the deposited analyte from the working electrode surface while generating an anodic faradaic current that is related to the analyte concentration in the sample.

In this work, we report the use of gold (Au)-based sensor for determination of Hg by ASV. We recently reported the use of a platinum (Pt)-based sensor for determination of manganese (Mn) in drinking water [18,19]. However, the Pt working electrode (WE) is not suitable for Hg determination due to insufficient potential range. Thus, herein we use a gold WE, coupled with a gold auxiliary electrode (AE) and a Ag/AgCl reference electrode (RE). We demonstrated a calculated LOD of 15ppb in urine, which is well below the 50 ppb (μg/L) federal Biological Exposure Index (BEI) in the US [20]. The sensor was validated with de-identified healthy-donor urine samples. These results suggest that an electrochemical sensor based on Au can be a used in sensing system for rapid assessment of Hg exposure at point-of-care.

2 Experimental Methods

2.1 Chemicals and Reagents

Reagents were prepared using chemicals purchased from Fisher Scientific, if not stated otherwise. Trace metal grade hydrochloric acid (HCl) was diluted with deionized (DI) water to prepare the supporting electrolyte in a variety of concentrations (i.e., 0.01 M, 0.1 M, 0.2 M, 0.5 M, and 1 M). Sodium acetate buffers of two concentrations (0.1 M and 0.2 M) were prepared by dilution from a stock solution of 3.0 M, pH 5.2 ± 0.1 sodium acetate (Sigma-Aldrich, St. Louis, MO). Mercury solutions were prepared from an atomic absorption standard solution of 1000 mg/L Hg^{2+} in 12 % nitric acid (Acros Organics). Silver Cyless II RTU (Technic Inc., Cranston, RI) solution was used to electroplate Ag/AgCl reference electrodes. Electrochemical surface cleaning steps were performed with a sulfuric acid (H_2SO_4) solution (36 N, 18 M) diluted with DI water to 0.05 M. Sodium hydroxide (NaOH) pellets 99.99 % trace metals basis (Sigma Aldrich) were mixed with DI water to form 1 M and 5 M NaOH solutions that were used to adjust the pH of urine samples.

2.2 Sensor and Instrumentation

Thin-film gold electrode sensors in this study were procured from Micrux Technologies (Oviedo, Spain). The sensors (ED-SE1-Au) are based on a three-electrodes configuration on a glass substrate. The working electrode (WE) is a circle of 1 mm diameter, with semi-circular counter electrode (CE) and reference electrode (RE). All electrodes were formed by a 150 nm thick Au layer, on top of a 50 nm Ti adhesive layer. The Au RE was transformed into an Ag/AgCl RE by electroplating in a two-step process. First, Ag was plated onto the Au RE with a cathodic current (3 mA/cm^2) for 240 s, and then chloridized with anodic current (3 mA/cm^2) for 120 s in 1 M KCl. All three electrodes were confined by a protective layer of SU-8 resin, with a 2 mm circular opening to delimit the cell area. The overall sensor substrate was a 10×6 mm^2 rectangle made of glass (0.75 mm thick) with an SU-8 resin protective layer to allow use of small sample volume (droplet).

Thin-film Au sensors need both electrochemical and physical cleaning steps. Electrochemical surface cleaning procedure activates the electrodes surface by generating hydrogen and oxygen and removing any oxides or chemical residues left from production. For this purpose, 0.05 M H_2SO_4 solution was used as background electrolyte in a cyclic voltammetry process between −1.0 V and +1.3 V at 100 mV/s sweep rate for 24 cycles. Physical cleaning helps remove particles or dust. This was done by rinsing each sensor with DI water for 20 s at room temperature and then drying with a 10 s jet of compressed air. While electrochemical cleaning was performed only once, at the beginning of each sensor life, before any other electrochemical procedure, physical cleaning was repeated in between every experiment to wash away solution residues.

In this work, WaveNow miniature USB potentiostat (Pine Instruments, Inc.) was used to perform all the electrochemical measurements and the AfterMath Data Organizer Software was employed. The All-in-One Platform from Micrux was used to interface the Au sensor and the potentiostat. Part of the experiments included a vibration motor in the system set-up. It is a flat coin button-type DC brushed motor in compact size (diameter 10 mm, thickness 2.7 mm), controlled using Arduino (Arduino UNO). The interface was appositely 3D-printed to accommodate the Au Micrux thin-film sensor, the vibration motor connected to Arduino, while still allowing connection through micro-USB to the potentiostat [19].

2.3 Sample Preparation

De-identified healthy single-donor urine samples were purchased from Innovative Research, Inc. (Novi, MI). The samples were stored in metal-free 15 mL conical

tubes. Each tube was frozen at −20 °C and defrosted when needed. Urine solutions were prepared by mixing the specimen and supporting electrolyte. Different amounts of Hg were spiked according to the experiment.

2.4 Analytical Procedure

Experiments were performed at room temperature (~18 °C) and with relative humidity of ~30 %. Room hygrothermal conditions were kept stable by a thermostat and they did not change throughout the year. The experimental procedure follows similar steps as our previous work [18]. Cyclic voltammetry (CV) and Square Wave Anodic Stripping voltammetry (SWASV) were performed to confirm the positions of the oxidation and reduction peaks of Hg. A cleaning step was included in the form of chronoamperometry between the measurements of Hg: a positive potential (+1.3 V) was applied to the sensor covered with mercury-free solution (mercury-free supporting electrolyte or mixture of the supporting electrolyte and mercury-free urine) to force stripping of possible mercury residues on the electrode. The experimental protocol of SWSV analysis was the following: 3 experiments in buffer mercury-free solution were performed as background, then 3 experiments were conducted for each mercury concentration. The cleaning step was performed between each of the experiments with mercury. All experiments performed on the same sensor were plotted together to identify the stripping peak of mercury with respect to the flat voltammogram of backgrounds. Concentrations ranged from 15 ppb to 200 ppb Hg in the buffer, from 5 ppb to 20 ppb Hg in urine. For each Hg concentration peak height and area in the voltammogram were calculated. Performance of the sensor, including limits of detection, accuracy and variability, were determined and optimized through experimental parameters and contact interface. Best ionic strength and composition of the supporting electrolyte solution were investigated as well. We confirmed the validity of the point-of-care system by performing and optimizing the electrochemical analysis using human specimens. The limit of detection (LOD) was calculated both in buffer and in urine following the 3σ/slope approach [21]. Detection capabilities of the designed system were confirmed with blind tests on the detection of spiked Hg (0 ppb, 5 ppb, 10 ppb, 15 ppb) in urine. Standard addition applied to certified urine samples was used to reach this purpose.

3 Results and Discussion

3.1 Optimization of ASV Conditions

The experimental conditions were thoroughly investigated and optimized. First, two supporting electrolytes were selected based on literature suggesting that acidic environment is desirable for Hg determination: 0.1 M sodium acetate buffer (pH 5.2) [22] and 0.1 M hydrochloric acid (HCl) [23]. We used cyclic voltammetry (CV) to compare these two electrolytes by obtaining their potential windows, while addition of 10 ppm Hg^{2+} was used to locate the reduction peaks. Background scans in Figure 1a show a large anodic current above 0.7 V, which is attributed to oxide formation on the Au electrode. A large cathodic current due to hydrogen evolution on the Au electrode occurs below 0 V (not shown), so the scan was terminated at 0 V to prevent damaging electrodes. Thus, both electrolytes exhibit a potential window of ~700 mV.

Oxidation and reduction peaks of Hg^{2+} are clearly visible in both electrolytes. In HCl electrolyte, the potential of the oxidation peak is ~500 mV and the reduction peak is ~480 mV. Aside from the reduction and oxidation peaks, the voltammogram with Hg overlaps well with the background voltammogram. In addition, the background signal remains relatively flat at the peak potential making peak evaluation straightforward. In acetate buffer, however, there is a strong background signal at the peak potential which would reduce sensitivity, and broad peak shape would make its evaluation less straightforward. Thus, based on the shape of the Hg peak and the flatness of the background signal, HCl electrolyte was selected for further analysis.

Next, we used CV to examine the impact of the HCl electrolyte ionic strength on the background signal and ultimately the Hg peak shape. Figure 1b illustrates voltammograms for HCl electrolyte of various ionic strengths, from 0.01 M to 1 M. As ionic strength increased, the background waveform exhibited a progressively stronger signal that appears as a pair of broad peaks. A strong background signal can reduce sensitivity and is undesirable; thus a 0.01 M and 0.1 M electrolytes were preferable for this work since its signal remained relatively flat. Figure 1c illustrates ASV over a more restricted potential range. We scanned background of both 0.1 M and 0.01 M HCl electrolytes, as well as 30 ppb Hg^{2+} using 900 s deposition at 0 V for further comparison. The voltammograms in 0.01 M HCl (pH 2.5) were less regular and less flat than the ones in 0.1 M HCl (pH 0.1). Sensitivity and peak shape were similar, but the strong background signal of the 0.01 M HCl made it less desirable. Based on these comparisons, the 0.1 M HCl electrolyte was selected.

For stripping analysis, we examined time and potential of the deposition step since both strongly affect the reduction process of Hg. A 900 s deposition time was selected after a series of optimization experiments in which ASV deposition was varied from 600 s to 1500 s. The longer the time, the more analyte can reduce on the electrode surface and the higher will be the oxidation peak. However, if deposition lasts too long, the signal saturates, and analysis is unnecessarily time consuming. Figure 2a show that Hg reduction peak amplitude generally increases with time. To quantify these signals, we measured both peak amplitude and peak area. For peak area measurements, we performed baseline subtraction to adjust titled voltammograms horizontally to improve

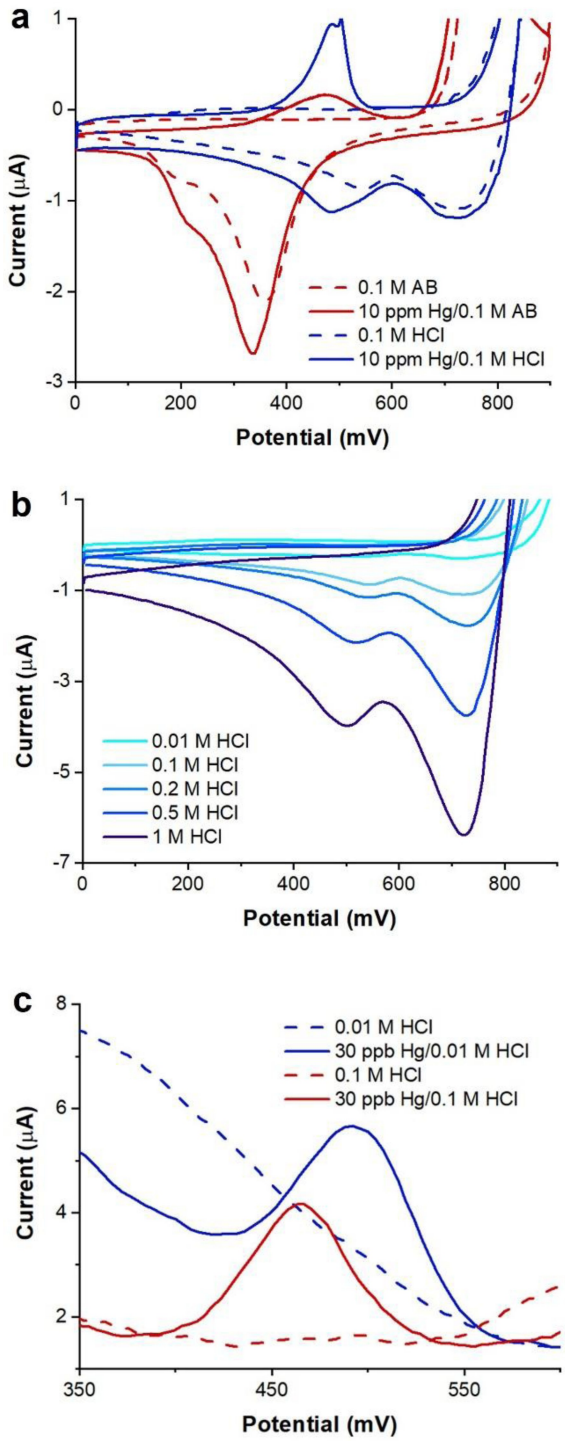

Fig. 1. Electrochemical performance of Au sensors in acetate buffer and HCl electrolyte. (a) CVs of the Au sensor in 0.1 M acetate buffer (AB) and 0.1 M HCl alone and with additional 10 ppm Hg to illustrate position and shape of Hg reduction and oxidation peaks. (b) CVs comparing performance of the Au sensor in HCl solutions of different ionic strength. (c) SWASV background scans in 0.01 M and 0.1 M HCl and with 30 ppb Hg to show the Hg stripping peaks.

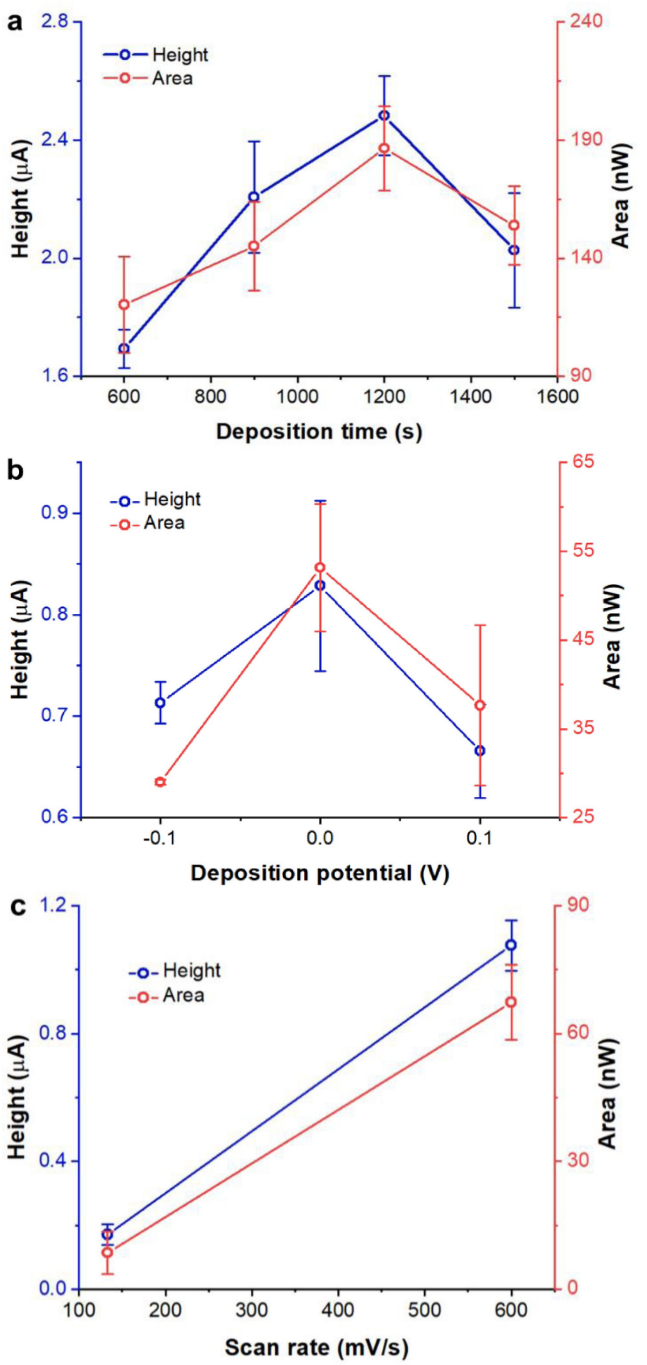

Fig. 2. Optimization of experimental parameters for Hg ASV by comparison of peak height (current) and area (power) of the Hg stripping peak. Optimization of (a) deposition time with 50 ppb Hg, (b) deposition potential with 20 ppb Hg, and (c) square wave scan rate (increment/period) with 15 ppb Hg.

accuracy. As Figure 2a illustrates, peak height tracks with peak area, and either measurement can be used for analysis quantification. The signal intensity is maximized at 1200 s, and it is comparable at 900 s and 1500 s. In most cases, voltammograms presented as a single but broad reduction peak at ~475 mV. The coefficient of variation (C.V.) of the signal remained consistent, in the 5–7 % range, regardless of the deposition time. Ultimately, although 1200 s deposition yielded a stronger signal, to

keep the analysis time manageable a 900 s deposition time was selected.

Investigation of the deposition potential, which also strongly impacts the reduction process of Hg, yielded an optimal value of 0 V. Figure 2b shows that with a deposition potential <0 V, there is a significant ~30 % drop in signal. While the more negative potential (relative to the stripping peak position) generally yields more efficient analyte deposition, the voltammograms show an increase in background signal, most likely due to a strong cathodic current. A similar, although smaller ~20 % drop in signal is observed with deposition potential >0 V, most likely due to less efficient deposition process.

In addition to the deposition time and potential, optimum waveform parameters for stripping by square wave voltammetry, including amplitude, period, increment and sampling width, were investigated using 0.1 M HCl spiked with 20 ppb Hg. Initially, the default Osteryoung settings [24,25] of 25 mV amplitude, 30 ms period, 5 mV increment, and 2 ms sampling width were used. However, the rate at which voltage changes over time (scan rate) influences the thickness of the diffusion layer [26] and, for faster scan rate, the diffusion layer decreases making it possible to measure higher faradaic currents (i.e., signal) while capacitive currents (i.e., noise) are reduced. For this reason, the scan rate was enhanced from 133 mV/s to 600 mV/s by decreasing the period of the square wave from 30 ms to 6 ms. Impact of this change is clearly visible in Figure 2c, which shows a nearly 6× signal enhancement. Ultimately, the Osteryoung square wave voltammetry parameters were optimized to 10 mV amplitude, 6 ms period, 4 mV increment, and 2 ms sampling width.

3.2 Calibration of Au Sensor in HCl

To demonstrate electrochemical performance, the Au sensor was calibrated in 0.1 M HCl using the optimized conditions. The concentrations ranged from 15 ppb to 200 ppb Hg, bracketing the BEI of 50 ppb. A series of representative voltammograms is shown in Figure 3a. After subtracting the baseline, we measured height (current) and area (power) of the Hg peak and plotted calibration curves for both (Figure 3b). The calibration curves show 99.5 % linearity between the Hg concentration and peak height or area. The correlation equation of peak height measurements is: I (μA) = 0.08 ([Hg(ppb)] - 0.72 (R^2 = 0.995, 6 data points), with 0.080 μA/ppb sensitivity. The limit of detection (LOD) is calculated as 3.1 ppb based on the 3σ/slope approach [21]. The correlation equation of peak area measurements is: P (nW) = 7.24 ([Hg(ppb)]) −114.4 (R^2 = 0.9953, 6 data points), with 7.2 nW/ppb sensitivity. The LOD is calculated as 3.6 ppb for peak area, which is less favorable than the calculation based on peak height. The limit of quantitation (LOQ) was 15 ppb Hg for both peak analysis methods. These values are higher than the previous reports of <1 ppb limits [23,27,28], but are sufficiently low for our target application; further, these prior studies were performed using bulk electrodes and thus are not a fair comparison to our miniaturized system.

3.3 Interferences

We performed a series of studies of metals that may potentially inference with Hg ASV, as real-world ASGM urine samples could contain other metals, and to ensure accurate and reliable determination of Hg. Different heavy metals were spiked into solutions with Hg to assess possible interferences. Based on literature [29–30], we selected several ions including As^{2+}, Pb^{2+}, Fe^{2+}, Zn^{2+} and Cu^{2+}. A 15 ppb Hg in 0.1 M HCl was used as control, while interfering metals were spiked in the ratios of 1:1, 1:10 and 1:100. The results show that none of these ions impact Hg stripping for ratios of 1:10 or below (Figure 4a–b). At 1:100, the Pb, Fe, Zi and As metals still did

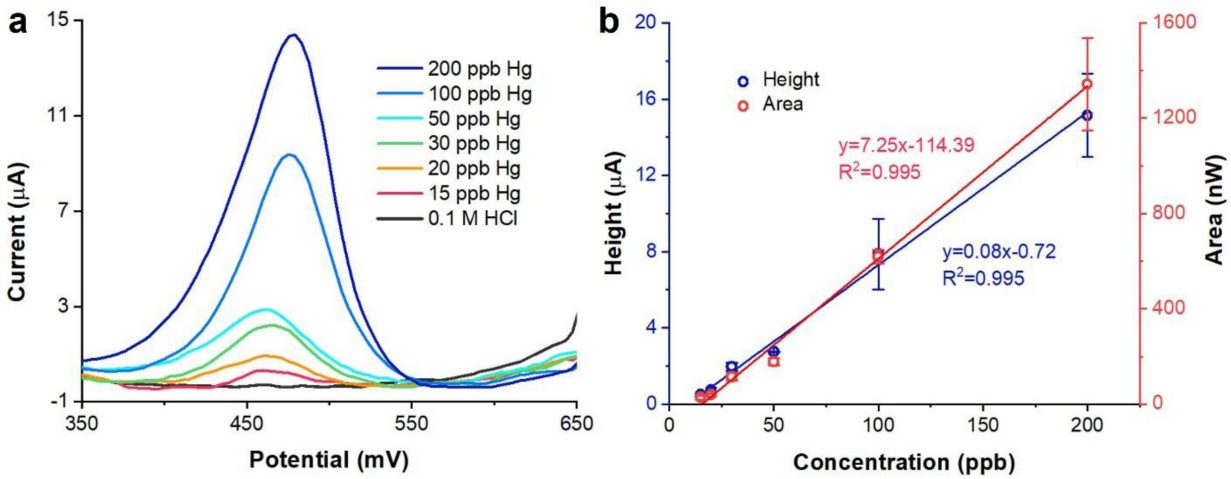

Fig. 3. Calibration of Au sensor. (a) Voltammograms in 0.1 M HCl under optimized conditions in 15–200 ppb Hg range, and (b) calibration plots of peak height and area.

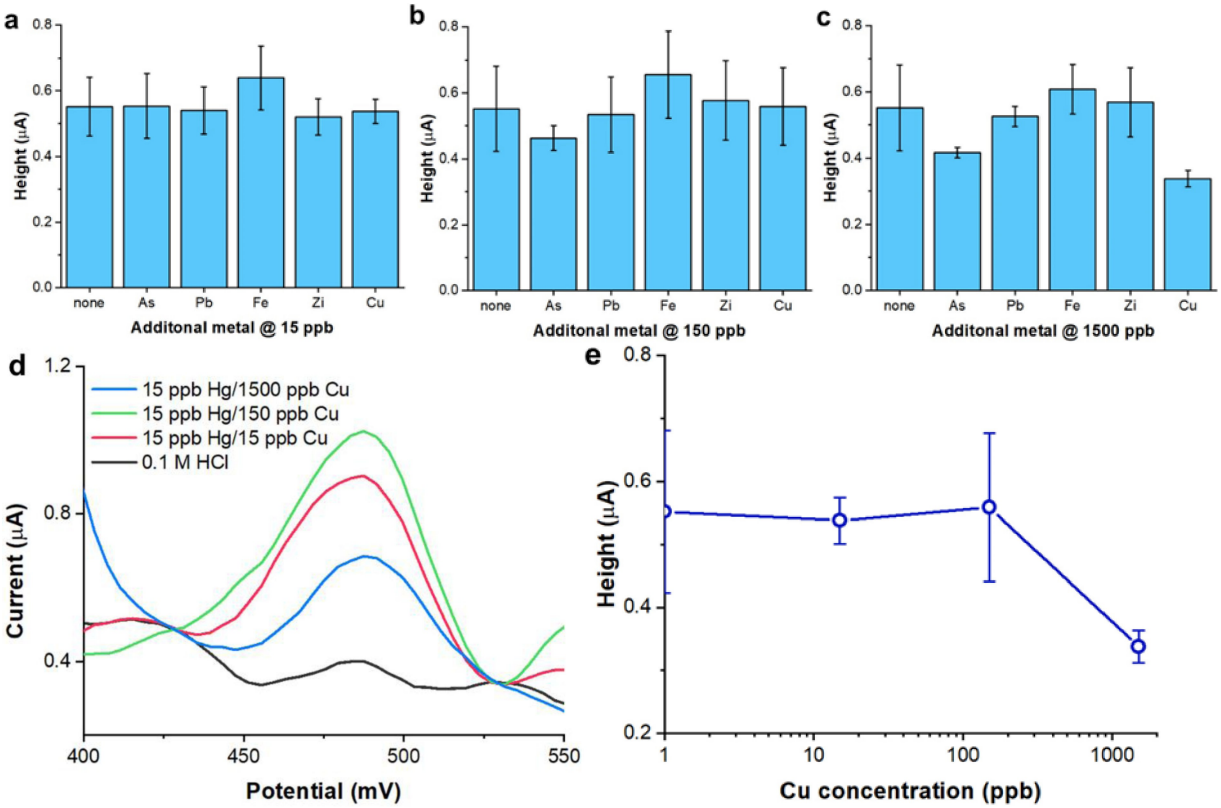

Fig. 4. Assessment of five metal interferences to Hg SWASV detection. (a) Measurement of 15 ppb Hg without added metal (control) and with addition of 15 ppb of arsenic, lead, iron, zinc, and copper. (b) Measurement of 15 ppb Hg without added metal (control) and with addition of 150 ppb of arsenic, lead, iron, zinc, and copper. (c) Measurement of 15 ppb Hg without added metal (control) and with addition of 1500 ppb of arsenic, lead, iron, zinc, and copper. (d) Voltammograms illustrating Hg measurements with increasing Cu concentration. (e) Peak height of Hg measurements with increasing Cu concentration.

not alter the measurements. However, presence of ppm level of Cu caused a drastic 50 % reduction in Hg signal intensity (Figure 4c). Examining the stripping waveforms (Figure 4d), it appears that presence of Cu does not adversely impact the waveform shape but rather depresses its height. Thus, an area-based analysis would not be beneficial. Plotting peak height for determination of 15 ppb Hg as a function of increasing concentration of Cu, signal clipping becomes obvious when Cu levels exceed 150 ppb (Figure 4e). This is somewhat analogous to the interference we observed from iron in determination of Mn in our prior work [18]. The normal Cu range in human urine is 20–50 μg/24 h (10–25 ppb for a 2 L in 24 h urinary excretion) [31]. The results of this analysis show that high concentrations of Cu could interfere with Hg detection in urine samples with Au sensor but, while >50 ppb or ppm levels of Cu require immediate attention in every situation, for the specific case of ASGM, studies showed that there was no change in urinary Cu excretion after exposure to mercury vapors [32].

3.4 Determination of Hg in Urine

The sensor was used to demonstrate determination of Hg in urine samples. To improve performance of the sensor in urine samples, a vibration motor was included in the experimental setup. The vibration produces agitation and convection motion that increase sensitivity by disrupting the diffusion layer. We have recently used this approach to successfully improve detection limits in a study of Pt microelectrode for determination of manganese in drinking water [19]. Since the organic matrix of biological samples usually affects electrochemical analysis [33], samples must be first acidified with HCl. Thus, we began by investigating how much dilution was necessary for successful analysis. A dilution factor (DF) parameter, defined as a volumetric ratio of total volume (HCl electrolyte and urine sample) to urine sample, was used to determine dilution quality. A DF = 4 resulted in the best option for urine samples, but other values were investigated as well. Figure 5a compares voltammograms of 15 ppb Hg at different DF. A DF = 1 was attempted, but the organic matrix in urine had a strong effect and background and Hg voltammograms were noisy and the signal was not distinguishable. A DF = 8 helped reduce the organic matrix influence, with flatter background signal, but the 15 ppb Hg signal was barely identifiable. The pH value of the urine solution was also optimized. The pH values of 0.7, 2, 3.5, 6.5, and 10 were achieved by adding different volumes of trace level 0.5 M NaOH.

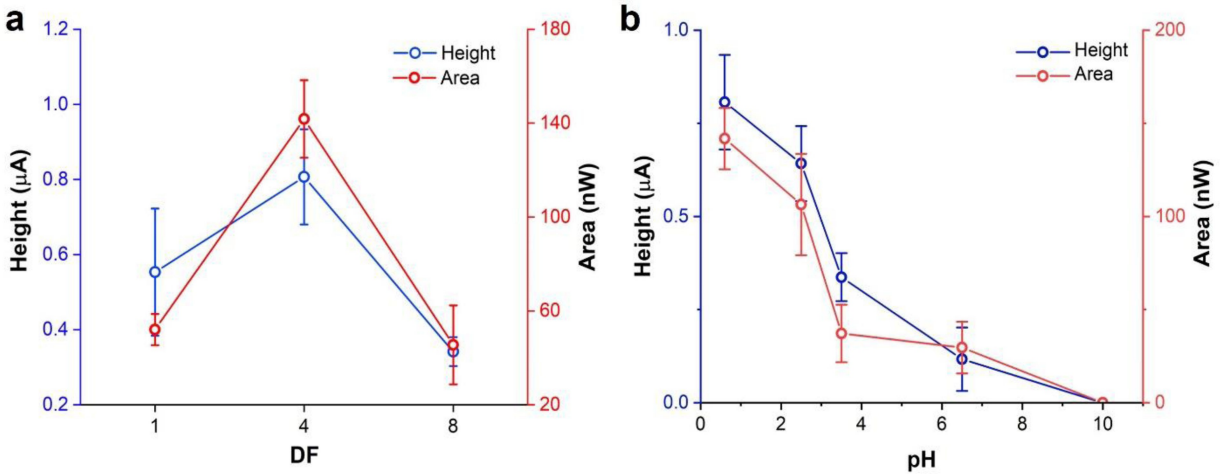

Fig. 5. Optimization of SWASV in urine. (a) Comparison of SWASV electrochemical performance at different urine dilution ratios (DF 1, 4 and 8) with addition of 15 ppb Hg. (b) Optimization of sample pH for measurement of 15 ppb Hg in urine.

15 ppb Hg was then spiked into the solutions for SWASW measurements. As shown in Figure 5b, the SWASW peak height and area of 15 ppb Hg keeps decreasing with pH, and pH of 0.7 shows the highest signal. Thus, 0.7 was chosen as the optimal pH value.

After the optimization of the dilution factor and the pH value, the calibration curve was built with successful measurement of spiked samples in the 5 ppb to 20 ppb range. Considering the dilution factor of 4, the mercury concentration in the urine should be 20 to 80 ppb range. The resulting stripping waveforms and calibration curve are shown in Figure 6. As shown in Figure 6a, the peak of Hg in the urine solution is much broader than that in the supporting electrolyte, which makes finding the peak height more difficult, thus the area measurement was considered a better analysis approach for determination of Hg in urine. Figure 6b shows the calibration curve of the peak area and the correlation equations: P (nW) = 14.79 ([Hg(ppb)]) −24.79 (R^2 = 0.96, 4 data points). The calculated LOD is 3.8 ppb for peak area (sensitivity 14.8 nW/ppb).

To further assess reproducibility of the sensor and determine precision of the approach, ASV was performed with 10 ppb Hg in urine solution on six sensors, replicating each measurement 3× times. Peak area and the variation coefficient are reported in Figure 7. Peak area ranges from ~125 nW to ~180 nW. The maximum coefficient of variation is 16 %, with an average of 10 %. This demonstrates that the thin-film Au sensor can measure Hg in biological sample with precision of approximately 90 %.

Urine samples were investigated with a standard addition technique to test the efficacy of the system in detecting unknown concentrations of mercury. Five different samples were used for this purpose. Three different known concentrations were added (5, 10, 15 ppb Hg) plus

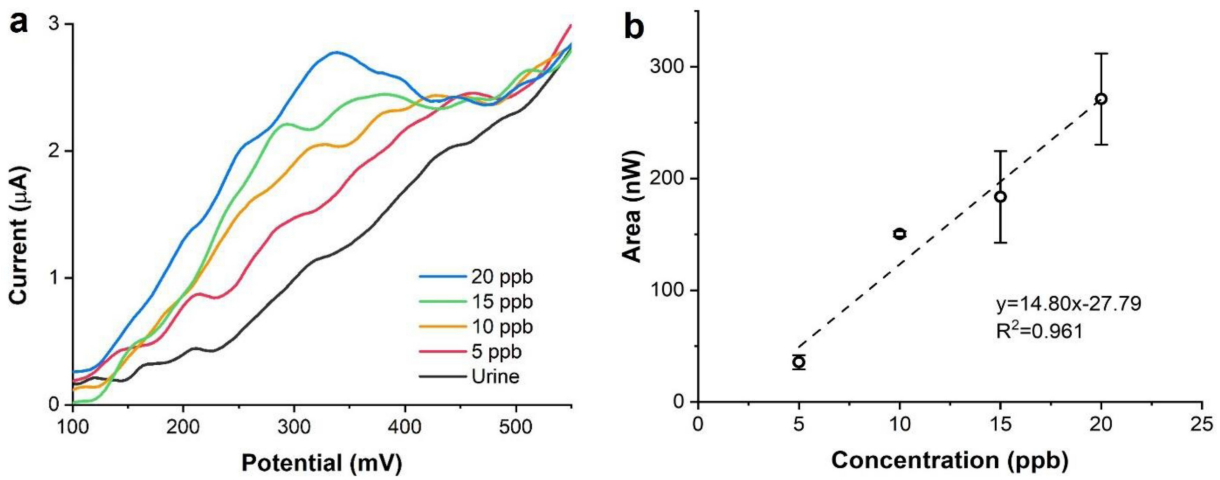

Fig. 6. (a) Voltammograms of calibration of Au sensor in urine under optimized conditions in the 5–20 ppb Hg range, and (b) calibration plots of peak area in urine.

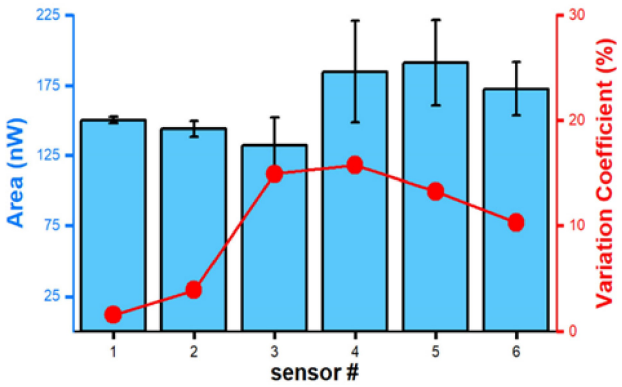

Fig. 7. Representative SWASV measurements in urine (10 ppb Hg with 6 different sensors). Comparison of peak area and its coefficient of variation.

an unknown concentration spiked in the solutions by a lab member. The representative voltammograms show that the shape of the peaks is adherent to the optimization experiments. A representative plot of standard addition is given in Figure 8. The calibration curve of the peak area of the standard addition experiment is given as: P (nW) = 18.4 ([Hg(ppb)]) + 89.13 (R^2 = 0.99, 4 data points). The sensitivity is similar to the previous calibration in urine. Five samples were measured with the SWASV standard addition experiments. The results of measured value and the accuracy are reported in the Table 1. Accuracy is calculated as the agreement between the SWASV measurement and the real concentration. Based on the results in Table 1, the average accuracy of the SWASV approach is 86.6 % and the Pearson's correlation is 0.95, which illustrate the high accuracy of our SWASV approach of measuring Hg.

4 Conclusions

In this work, mercury assessment was obtained by SWASV with thin-film Au sensors. This system succeeded in detecting trace concentrations of mercury both in the supporting electrolyte and urine sample. A 15 ppb Hg and 5 ppb Hg respectively in 0.1 M HCl and urine are the limits of quantitation. The lowest limits of detection are 3.1 ppb Hg in peak height measurements in supporting electrolyte solution and 3.8 ppb Hg in area measurements in urine solutions (15 ppb Hg considering the dilution factor). It measured amounts of mercury below the BEI threshold of 50 ppb Hg, which represents the intervention level established by the US federal government. This will allow early intervention among people in ASGM industries in developing countries, where mercury is used to extract gold from ore sediments and inhalation of mercury fumes can result in severe poisoning. The designed system is suitable for POC applications that can identify mercury intoxication, even at early stages, without the need of long analysis in big laboratories. The advantages of this miniature system are the use of disposable sensors and a

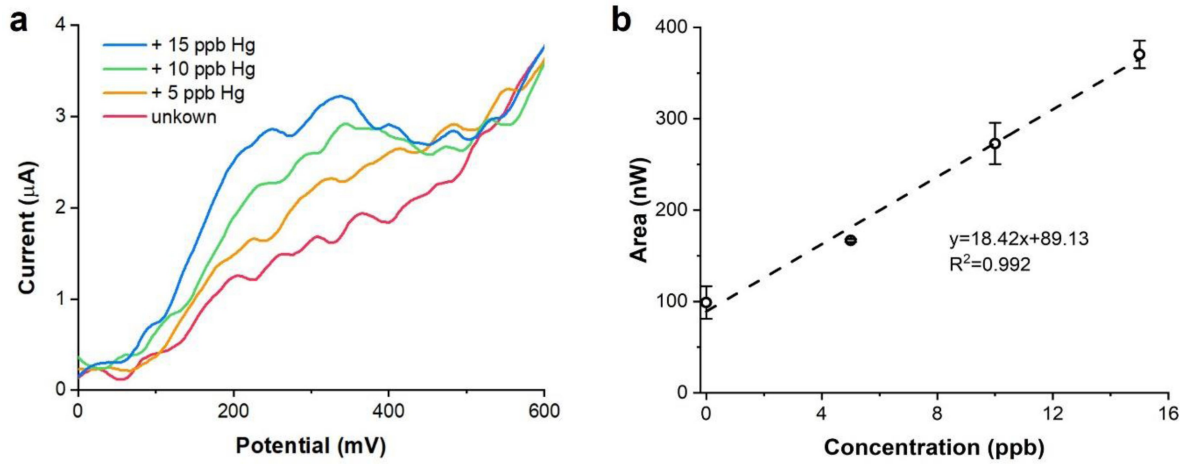

Fig. 8. (a) Representative waveforms of the standard addition experiment. (b) Standard addition plot of peak area. The original concentration of Hg in the urine sample can be calculated using the equation in (b) and the dilution factor.

Table 1. Results of five different standard addition experiments with accuracy.

Sample #	Spiked Concentration [ppb]	SWASV measurement results [ppb]	Accuracy area [%]
1	5.0	4.8	96.0
2	6.5	5.0	76.9
3	5.0	4.5	88.0
4	8.0	9.6	80.0
5	10.0	10.8	92.0

portable instrument, rather than an expensive laboratory-based system.

Acknowledgements

This work was supported in part by funds provided by the National Institute for Occupational Safety and Health award T42OH008672 and by the National Institutes of Environmental Health and Sciences (NIEHS) award R33ES024717. Its contents are solely the responsibility of the authors and do not necessarily represent the official views of NIOSH or NIEHS.

Data Availability Statement

The data that support the findings of this study are available from the corresponding author upon reasonable request.

References

[1] H. Cossa, R. Scheidegger, A. Leuenberger, P. Ammann, K. Munguambe, J. Utzinger, E. Macete, M. S. Winkler, *Int. J. Environ. Res. Public Health* **2021**, *18*, 1.
[2] H. Gibb, K. G. O'Leary, *Environ. Health Perspect.* **2014**, *122*, 667.
[3] WHO, Prev. Dis. Healthy Environ. **2006**, 4.
[4] J. D. Park, W. Zheng, *J. Prev. Med. Pub. Health* **2012**, *45*, 344.
[5] G. Sandborgh-Englund, C. G. Elinder, S. Langworth, A. Schütz, J. Ekstrand, *J. Dent. Res.* **1998**, *77*, 615.
[6] L. A. Broussard, C. A. Hammett-stabler, R. E. Winecker, *Lab. Med.* **2002**, *33*, 614.
[7] K. M. Bose-O'Reilly, Stephan, *Brain Behav. Immun.* **2008**, *22*, 4109.
[8] F. Jonsson, G. Sandborgh-Englund, G. Johanson, *Toxicol. Appl. Pharmacol.* **1999**, *155*, 161.
[9] S. R. Kolrtyohann, M. Khalil, *Anal. Chem.* **1976**, *48*, 136.
[10] W. Geng, T. Nakajima, H. Takanashi, A. Ohki, *J. Hazard. Mater.* **2008**, *154*, 325.
[11] B. Passariello, M. Barbaro, S. Quaresima, A. Casciello, A. Marabini, *Microchem. J.* **1996**, *54*, 348.
[12] S. A. Winfield, N. D. Boyd, M. J. Vimy, F. L. Lorscheider, *Clin. Chem.* **1994**, *40*, 206.
[13] M. Gallignani, H. Bahsas, M. R. Brunetto, M. Burguera, J. L. Burguera, Y. Petit de Peña, *Anal. Chim. Acta* **1998**, *369*, 57.
[14] B. M. W. Fong, S. S. Tak, J. S. K. Lee, S. Tam, *J. Anal. Toxicol.* **2007**, *31*, 281.
[15] J. S. Tsuji, P. R. D. Williams, M. R. Edwards, K. P. Allamneni, M. A. Kelsh, D. J. Paustenbach, P. J. Sheehan, *Environ. Health Perspect.* **2003**, *111*, 623.
[16] H. A. Strobel, W. R. Heineman, *Chemical Instrumentation: A Systematic Approach, 3rd Edition*,, Wiley, **1989**.
[17] P. T. Kissinger, W. R. Heineman, *Laboratory Techniques in Electroanalytical Chemistry, 2nd Edition*, CRC press, **1996**.
[18] W. Kang, C. Rusinek, A. Bange, E. Haynes, W. R. Heineman, I. Papautsky, *Electroanalysis* **2017**, *29*, 686.
[19] E. Boselli, Z. Wu, A. Friedman, B. Claus Henn, I. Papautsky, *Environ. Sci. Technol.* **2021**, *55*, 7501.
[20] R. A. Bernhoft, *J. Environ. Public Health* **2012**, *2012*, 460508.
[21] D. A. Armbruster, T. Pry, *Clin. Biochem.* **2008**, *29*, 49.
[22] I. A. Tayeb, K. Abdul Razak, *J. Phys. Conf. Ser.* **2018**, *1083*, 0.
[23] A. Mandil, L. Idrissi, A. Amine, *Microchim. Acta* **2010**, *170*, 299.
[24] J. Osteryoung, *Electroanal. Methods* **1985**, *1*, 121.
[25] C. A. Rusinek, W. Kang, K. Nahan, M. Hawkins, C. Quartermaine, A. Stastny, A. Bange, I. Papautsky, W. R. Heineman, *Electroanalysis* **2017**, *29*, 1850.
[26] N. Elgrishi, K. J. Rountree, B. D. McCarthy, E. S. Rountree, T. T. Eisenhart, J. L. Dempsey, *J. Chem. Educ.* **2018**, *95*, 197.
[27] A. Giacomino, O. Abollino, M. Malandrino, E. Mentasti, *Talanta* **2008**, *75*, 266.
[28] Y. Bonfil, M. Brand, E. Kirowa-Eisner, *Anal. Chim. Acta* **2000**, *424*, 65.
[29] S. Kebenei, *J. Environ. Earth Sci.* **2020**, *10*, 144.
[30] N. A. Gafur, M. Sakakibara, S. Sano, K. Sera, *Water Switz.* **2018**, *10*, 1.
[31] T. Lech, J. K. Sadlik, *Biol. Trace Elem. Res.* **2007**, *118*, 16.
[32] G. Sällsten, L. Barregård, Biometals *Int. J. Role Met. Ions Biol. Biochem. Med.* **1997**, *10*, 357.
[33] Matrix Effect, *IUPAC Compend. Chem. Terminol.* **2008**, *2243*, 3759.

Received: May 21, 2022
Accepted: July 29, 2022
Published online on August 18, 2022

